Partially Pyrolyzed Poly(dimethylsiloxane)-Based Networks: Thermal Characterization and Evaluation of the Gas Permeability

NÁDIA M. JOSÉ,[1] LUIS A. S. DE ALMEIDA PRADO,[2] MARCO A. SCHIAVON,[3,4] SIMONE U. A. REDONDO,[3] INEZ V. P. YOSHIDA[3]

[1]Instituto de Química, Universidade Federal da Bahia, Campus de Ondina, Salvador-BA, Brazil

[2]Institute of Polymers and Composites, Technische Universität Hamburg–Harburg, Hamburg, Germany

[3]Instituto de Química, Universidade Estadual de Campinas, Campinas-SP, Brazil

[4]Departamento de Ciências Naturais, Universidade Federal de São João del Rei, São João Del Rei-MG, Brazil

Received 25 September 2006; revised 30 October 2006; accepted 6 November 2006
DOI: 10.1002/polb.21053
Published online in Wiley InterScience (www.interscience.wiley.com).

ABSTRACT: In this investigation, the preparation and characterization of partially pyrolyzed membranes based on poly(dimethylsiloxane) (PDMS) are described. These membranes were obtained by the crosslinking of silanol-terminated PDMS with multifunctional nanoclusters derived from the reaction of pentaerythritoltriacrylate with 2-aminoethyl-3-aminopropyltrimethoxysilane and the *in situ* polycondensation of tetraethylortosilicate, followed by the thermal treatment of the resulting membranes at different temperatures. The partially pyrolyzed membranes were characterized with infrared spectroscopy, thermogravimetry, elemental analyses, dynamic mechanical analysis, small-angle X-ray scattering, and scanning electron microscopy. The membranes exhibited improvements in the thermal stability and mechanical strength. Even with distinct compositions with respect to the Si/O and Si/C ratios, the flexibility of these materials was maintained. The flux rates of the gases through the membranes were measured for N_2, H_2, O_2, CH_4, and CO_2, at 25 °C. The permeability of the membranes changed with increases in the pyrolysis and oxidation temperatures. These membranes could be described as PDMS chains separated by inorganic clusters. ©2006 Wiley Periodicals, Inc. J Polym Sci Part B: Polym Phys 45: 299–309, 2007
Keywords: crosslinking; mechanical properties; networks; polysiloxanes; thermogravimetric analysis (TGA)

INTRODUCTION

Polyorganosiloxanes are a class of polymers that have attracted the interest of many researchers because of their versatility for tailoring materials with different properties.[1] Some of the emerging applications of polysiloxane-containing materials include their pyrolytic conversion in ceramic bodies[2–5] and their use as membranes for different applications.[6–15]

The utilization of polysiloxanes in the last decades in materials science has been advantageous because of the variety of precursor monomers, oligomers, and polymers with different functional organic groups, which make easier the preparation of materials with different architectures and properties. Poly(dimethylsiloxane) {PDMS or $[Si(CH_3)_2O]_n$} is by far the most

Correspondence to: N. M. José (E-mail: nadia@ufba.br)
Journal of Polymer Science: Part B: Polymer Physics, Vol. 45, 299–309 (2007)

known and used polymer of its category. This polymer has one of the lowest glass transitions[16] and highest gas permeability coefficients.[17] The crosslinking of linear PDMS chains to produce elastomeric networks can be performed by different processes, such as (1) γ radiation, (2) radical initiators, (3) polycondensation reactions of —Si$(CH_3)_2$OH end groups with silicon alkoxides, and (4) addition reactions such as hydrosilylation.[18–22]

Because PDMS-based membranes have high permeability to gases, they have been considered for gas-separation processes.[23] Because of the relatively low selectivity coefficients exhibited by these membranes, studies focused on tailoring the gas-transport properties of polysiloxane membranes, through the control of their molecular architecture, have been developed.[24]

The development of membranes with good performance for use in high-temperature gas-separation processes is still a challenge. Research in this area has often focused on inorganic materials and molecular sieves because of their promising applications under severe conditions, such as high temperatures and pressures.[25,26]

Alternatively, porous ceramic membranes offer high transport rates but reduced selectivity coefficients.[27] Koresh and Soffer[28] described the preparation of carbon molecular sieve membranes formed by the pyrolysis of organic material. These membranes showed high selectivity coefficients for H_2/CH_4. Stevens and Rezac[29,30] developed highly thermally stable membranes, using the controlled partial pyrolysis of polymeric films as an alternative route.

In organic–inorganic hybrid materials, the control of the temperature and time of the heat treatment under an inert atmosphere can promote the partial degradation of the organic component, with the maintenance of the polymeric characteristic of the material. On the other hand, this partial pyrolysis under an oxidative atmosphere can promote additional crosslinking of the polymeric chains, which contributes to the decrease in the free volume and the increase in the hardness of the final material.[29]

Among several methods, the partial and controlled pyrolysis of PDMS-based membranes is a relatively easy process to increase the amount of an inorganic component in the membranes by the partial removal of organic functional groups, producing materials with improved thermal stability.

In this work, partially pyrolyzed membranes were prepared through the controlled pyrolysis of PDMS-based films, which were obtained from PDMS crosslinked with alkoxide-functional clusters, containing an organic core. These clusters were prepared by the reaction of pentaerythritoltriacrylate (PETA) and 2-aminoethyl-3-aminopropyltrimethoxysilane (AS) and silica oligomers. The resulting membranes were characterized with Fourier transform infrared (FTIR) spectroscopy, X-ray diffraction (XRD), small-angle X-ray scattering (SAXS), thermogravimetric analysis (TGA), dynamic mechanical analysis (DMA), and elemental analysis (C, H, N, and Si). The morphology of the membranes was investigated with field emission scanning electron microscopy (FESEM). The permeability coefficient and ideal selectivity coefficient were evaluated for O_2, N_2, H_2, CH_4, and CO_2 gases. The characterization results as well as the evaluation of the thermal and gas-transport properties of these films are discussed.

EXPERIMENTAL

Materials

PDMS with a numeric average molecular weight of 2200 g/mol, AS, and tetraethoxysilane (TEOS) were supplied by Dow Corning. The trifunctional acrylic monomer, PETA, was obtained from Aldrich Chemical Co. The dibutyltin–dilaurate complex (5 wt % in hexane; Sn catalyst) was purchased from Gelest. 2-Propanol (99%) was purchased from Grupo Química (Brazil). AS was distilled under reduced pressure before use.

PDMS-Based Membranes

Homogeneous, transparent, self-supported, and crack-free PDMS films were prepared by the polycondensation reaction of linear PDMS containing Si—OH end groups with PETA/AS and TEOS. The 9-functional precursor, PETA/AS, was generated *in situ* by Michael addition between PETA and AS with a 1:3 molar ratio (see eq 1), as reported in our previous publications:[31]

$$\begin{aligned}&(HO)CH_2C(CH_2OCOCH{=}CH_2)_3(PETA)\\&\quad+H_2N(CH_2)_2NH(CH_2)_3Si(OCH_3)_3(AS)\\&\qquad\rightarrow(HO)CH_2C[CH_2OCOCH_2CH_2HN\\&\quad\times(CH_2)_2NH(CH_2)_3Si(OCH_3)_3]_3(PETA/AS)\end{aligned}\tag{1}$$

A solution of PDMS, PETA/AS, and TEOS (8:1:1 weight ratio) in 2-propanol was stirred at 40 °C

Table 1. Conditions Used for the Partial Pyrolysis of MPP1

Membrane	Purge Temperature (°C)	Oxidation Temperature (°C)
MPP2	150	100
MPP3	200	150
MPP4	250	200
MPP5	300	250

in the presence of dibutyltin dilaurate for 30 min. The viscous solution was transferred to Petri dishes, giving rise to transparent films after 72 h. These films were postcured *in vacuo* at 50 °C for 48 h. More experimental details are given elsewhere.[31] This material was coded MPP1. After a drying step, the membrane thickness ranged from 0.8 to 1.1 mm.

Partial Pyrolysis of MPP1

The partial pyrolyses of MPP1 were conducted by a heat treatment in both argon and synthetic air flowing atmospheres (100 mL/min) at different final temperatures (see Table 1). The pyrolysis was carried out by the placement of the sample in an alumina crucible and then in a tubular furnace at a heating rate of 2 °C/min with a holding time of 3 h at a specific purge temperature under an argon atmosphere; this was followed by cooling to 50 °C at a rate of 2 °C/min and then heating at a specific oxidation temperature under synthetic air for 3 h more. Finally, the samples were cooled at a rate of 2 °C/min. The changes in weight were controlled by the weighing of the samples before and after the pyrolysis cycle.

Methods

Infrared Spectroscopy

Infrared spectra were recorded with a Perkin Elmer 1600 FTIR spectrometer with the conventional KBr pellet in the transmission mode; 32 scans were recorded with a resolution of 4 cm^{-1}.

TGA

The thermogravimetry of the samples was carried out by the loading of ~10 mg of the samples into a TA 2950 thermobalance instrument under an argon atmosphere (100 mL/min flow rate), at 20 °C/min, from 30 to 1000 °C. The ceramic yield of each membrane was determined by the amount of the residue obtained at 1000 °C.

DMA

The dynamic mechanical behavior of these materials was analyzed with a TA Instrument DMA 983, in a tension mode and at a fixed frequency (1 Hz), in the range of −150 to 200 °C, at a scanning rate of 5 °C/min. The glass-transition temperature (T_g) here is defined as the temperature at which the material has the maximum loss modulus value.

Elemental Analysis

The carbon, hydrogen, and nitrogen contents in the partially pyrolyzed membranes were quantitatively measured in an elemental analyzer (model 2400, PerkinElmer) with a procedure suggested in previous publications.[32] The Si content was evaluated by X-ray fluorescence with an energy-dispersive X-ray spectrometer (model EDX700, Shimadzu) with a cellulose filter. The oxygen amount was estimated by difference. The errors estimated in these analyses were 5%. The results were displayed in terms of the Si/O and Si/C ratios.

SAXS

SAXS experiments were carried out at Soft Condensed Matter Beamline A2 at HASYLAB (Hamburg, Germany) with a fixed wavelength of 1.5 Å *in vacuo* at room temperature. The SAXS data were calibrated with the characteristics reflections of a rat tendon tail. Corrections due to the parasitic scattering (background) were performed after the measurement of each sample.

XRD

X-ray plots of the films were recorded on a Shimadzu XRD-600 diffractometer with Cu Kα radiation ($\lambda = 1.54$ Å).

Scanning Electron Microscopy

The morphology of the membranes was analyzed by FESEM with a JEOL JSM-6340F microscope operated at 3 kV. The observed surface was obtained by the coating of the cryogenic fracture with thin carbon and gold layers.

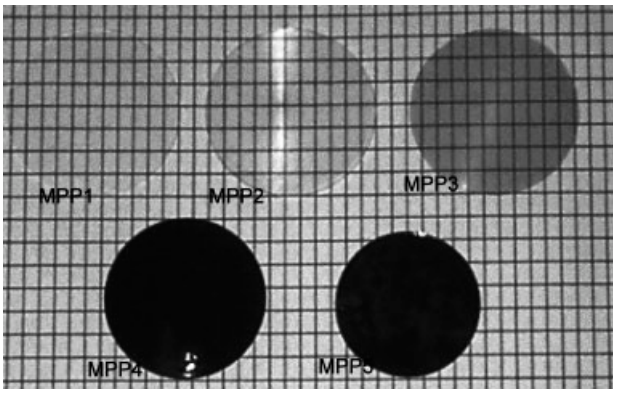

Figure 1. Photographs of the MPP*i* membranes.

Permeability Measurements

The gas permeability of the hybrid membranes was determined with a commercially available test cell (Gelman Science, Ann Arbor, MI), with pure H_2, N_2, O_2, CO_2, and CH_4 gases, at room temperature. The effective membrane area was 9.62 cm^2. The time lag was measured at least five times. The reproducibility of the data was checked by the measurement of at least four films (from the same batch) to avoid experimental errors due to eventual cracks. The ideal selectivity was obtained by the calculation of the ratio between the permeability values for different gases, as reported in our earlier publications.[12]

RESULTS AND DISCUSSION

Pyrolytic Treatment of the MPP1 Membrane

The membranes prepared with oxidative temperatures lower than 250 °C were transparent. After the thermal treatment, under different conditions, they became opaque (as illustrated in Fig. 1). The higher the temperature was of the thermal treatment, the higher the shrinkage was, as can be seen in Figure 1. The temperature of the maximum degradation rate, the shrinkage (%), the ceramic yield, and the Si/O and Si/C ratios for the prepared membranes are shown in Table 2. The more pronounced isotropic volume contraction and the higher ceramic yield were observed for the membranes treated at a higher temperature, as expected. Furthermore, the opaque and darker appearance of MPP4 and MPP5 can be associated with the partial degradation of the organic nucleus of PETA/AS clusters, which contain amino groups, by the heat treatment. The degradation of the ester group was already detected for poly(ethylene-*co*-vinyl acetate) at 200 °C under N_2.[33] When this polymer was heated under air, the formation of C—OH groups and oxidation to ketones and lactones, as well as the scission of C—C bonds, were observed at 250 °C.[33] In addition to the degradation of the organic nucleus of PETA/AS, the evolution of a volatile byproduct of the thermally induced condensations of residual silanol and alkoxide groups also contributed to the weight loss.

The pyrolytic conditions used in the preparation of MPP3, MPP4, and MPP5 were severe enough to cause redistribution reactions involving Si—O bonds in PDMS main chains, producing cyclic volatile siloxanes,[32,34] but not enough to cause redistributions of the nodes of the network.[35] In fact, the weight loss of MPP5 was ~20 wt %, which was higher than the PETA/AS core amount in this membrane, MPP5 was indeed brittle.

The elemental analysis of the partially pyrolyzed membranes showed an increase in the Si/C ratio with a concomitant decrease in the Si/O ratio. Moreover, the amounts of material eliminated after the pyrolysis (determined by the

Table 2. Temperature of the Maximal Decomposition Rate (T_{MAX}), Ceramic Yields, Shrinkage Values, and Elemental Analysis Ratios for the MPP*i* Membranes

Membrane	T_{MAX} (°C)	Ceramic Yield (%)	Shrinkage (%)	Elemental Analysis[a]	
				Si/C Ratio	Si/O Ratio
MPP1	543	20.2	—	0.50	1.48
MPP2	548	19.3	7.2	0.56	1.06
MPP3	547	20.9	13.5	0.67	1.02
MPP4	557	26.1	22.0	0.70	0.95
MPP5	559	47.8	66.4	0.75	1.19

[a] O was not analyzed. It was estimated by difference.

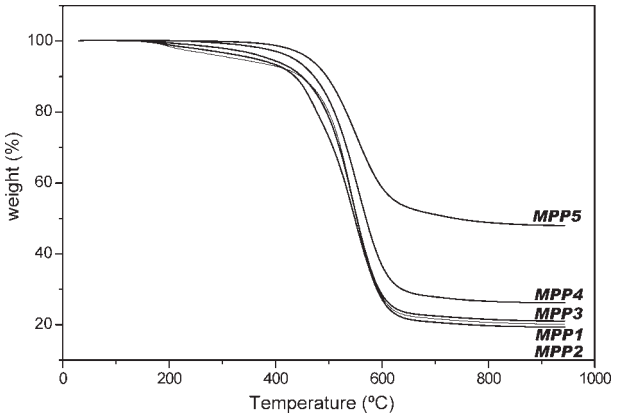

Figure 2. TGA curves of MPP1 and the partially pyrolyzed membranes (20 °C/min, Ar).

weighing of the membrane after and before the partial pyrolysis) were 2.7, 7.9, 20.2, and 68.8 wt % for MPP2, MPP3, MPP4, and MPP5, respectively.

No significant changes in the FTIR spectra of the membranes could be observed. These spectra were characteristic of PDMS-based materials, showing the principal absorptions at 1025 and 1007 cm^{-1}, characteristic of Si—O—Si stretching of relatively long —$[Si(CH_3)_2O]_n$— segments, as well as absorptions related to methyl groups at 2959 and 2926 (C—H stretching), 1260 (bending of C—H groups, fingerprint of Si—CH_3 groups), and 800 cm^{-1}.[36]

Thermal Behavior

Thermal Stability

Figure 2 contains the TGA curves of the MPP*i* membranes. The thermal degradation process of the membranes started at temperatures higher than the purge temperature, as expected. The onset temperature and the ceramic yield at 1000 °C increased in the order of MPP1 < MPP2 < MPP3 < MPP4 < MPP5 (Table 2), indicating an increase in the crosslinking density.

Interesting information could also be extracted from derivative thermogravimetric analysis (DTGA) curves. For MPP1 and MPP2 [Fig. 3(a)], two processes with T_{MAX}, defined as the temperature at which the mass flux from solid to vapor is maximum, were observed around 200 and 540 °C and could be clearly distinguished. The first stage could be assigned to the volatile evolution from the thermally induced condensation reaction involving residual ≡Si—OH and ≡Si—OC_2H_5 from PETA/AS and TEOS precursors.[31,34] The second one resulted from the degradation of the organic PETA/AS core in the nodes of the polysiloxane network and the structural rearrangements of the polysiloxane network.[32,34,35] Concerning the DTGA curves of the MPP3, MPP4, and MPP5 membranes [Fig. 3(b)], only the last degradation stage, with T_{MAX} between 547 and 559 °C, was observed. The rate of this process decreased in the order of MPP1 > MPP2 > MPP3 > MPP4 > MPP5. Taking into account the activation energies for the breaking of Si—O and Si—C bonds, 465 and 301 kJ/mol, respectively, we can conclude that the thermal degradation process observed here has considerable kinetic contributions rather then thermodynamic contributions, in agreement with Camino and coworkers[37,38] and Schiavon et al.[39] In fact, for a long PDMS chain, the activation energy involved in the degradation is far from the theoretical value of Si—O or Si—C bond cleavage

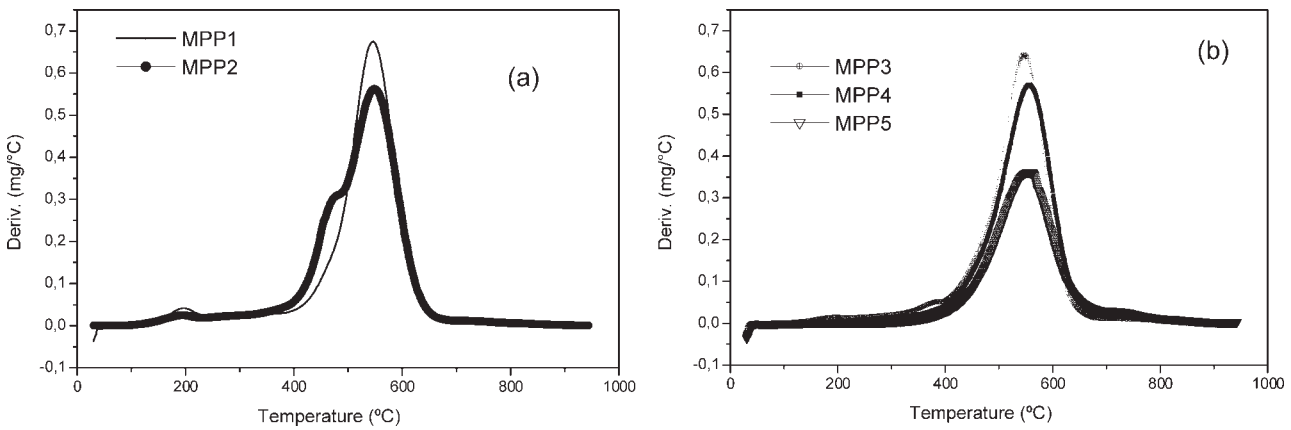

Figure 3. DTGA curves of the MPP*i* membranes: (a) MPP1, MPP2, and MPP3 and (b) MPP4 and MPP5.

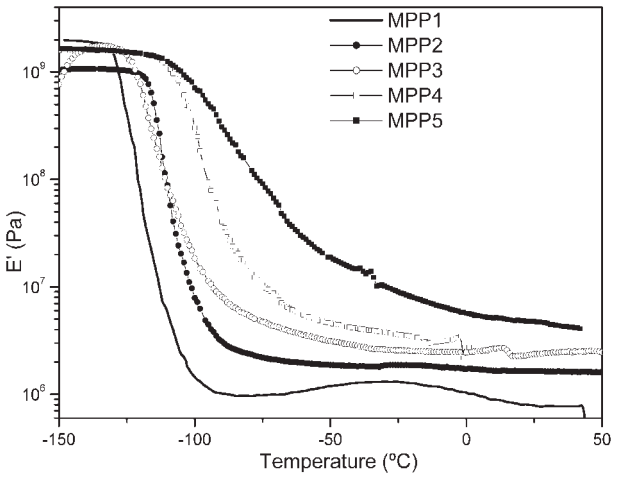

Figure 4. E' as a function of temperature for the MPP*i* membranes.

(190 kJ/mol) but is governed by kinetic considerations, which in turn are related to the molecular structure.[39]

It is well established that PDMS and polysiloxane copolymers and resins containing —Si$(CH_3)_2$O (or $D^{Me,Me}$) units undergo thermal degradation through the elimination of oligomeric cyclic products, as reported in several publications.[37–39] MPP4 and MPP5 showed evidence for the thermal degradation of the organic moieties of the PETA/AS as they became much darker than the previous ones. These oxidized species, not even detected in the FTIR spectra, may affect the degradation of these polysiloxane networks during the pyrolysis process.

DMA

Figure 4 shows the curves of the storage modulus (E') as a function of the temperature for MPP*i* membranes. At 25 °C, E' increased with an increase in the partial pyrolysis temperature because of the increase in the crosslinking density by the thermooxidation. The increase in E' in the viscoelastic regime was more evident for the MPP5 and MPP4 membranes.

The curves of the loss modulus (E''), illustrated in Figure 5, exhibited a maximum associated with the glass transition of the material. For MPP1, T_g was −120 °C. As the partial pyrolysis temperature increased, T_g values were shifted to higher temperatures and the transition became broader; this was in line with the increase in the crosslinking degree and also with the presence of structural heterogeneities, probably associated with the degradation of PETA/AS organic moieties. The T_g value increased as follows: MPP1 (−128 °C) < MPP3 (−121 °C) < MPP2 (−115 °C) < MPP4 (−106 °C) < MPP5 (−105 °C).

E' can also provide further evidence for the crosslinking of the pyrolyzed membranes through the determination of the average molecular weight between the nodes (M_C) of a polymeric network with the density (ρ) from E' at a temperature (T) higher than T_g, that is, in the viscoelastic regime, as illustrated by eq 2:[40,41]

$$E' = \frac{\rho \times R \times T}{M_C} \tag{2}$$

According to eq 1, membranes prepared at higher partial pyrolysis temperatures should have lower M_C values because these materials exhibit a higher E' value in the viscoelastic regime. In fact, lower M_C values can be correlated to the presence of shorter linear segments between the nodes. Therefore, MPP5 should have the lowest amount of PDMS. As the elimination of PDMS during the pyrolysis is expected to be more pronounced at higher temperatures, the increase in E' in the viscoelastic regime can be explained in terms of a decrease in M_C or, in other words, an increase in the crosslinking density.

XRD

The X-ray diffractograms of the partially pyrolyzed membranes were recorded to evaluate the structural changes induced by the thermal degradation of the MPP1 network. Figure 6 shows

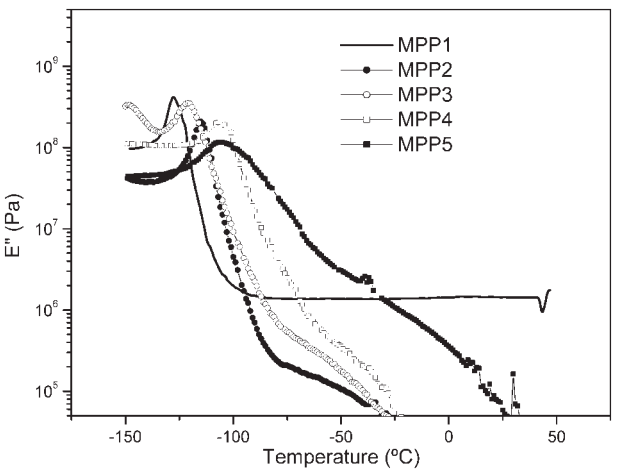

Figure 5. E'' as a function of temperature for the MPP*i* membranes.

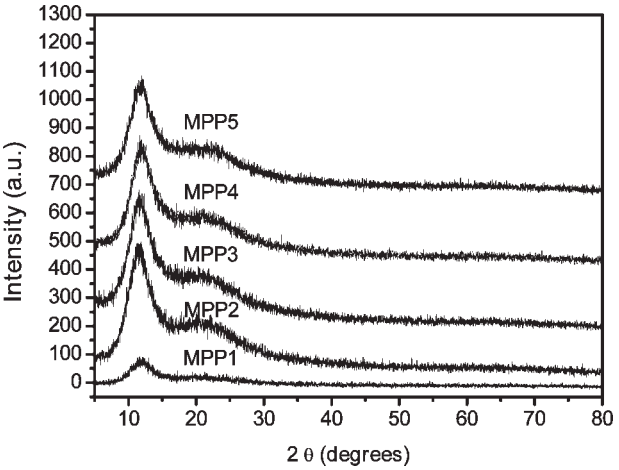

Figure 6. XRD plots of the partially pyrolyzed membranes (the curves have been shifted vertically for the sake of clarity).

the diffractograms of the studied membranes. All curves present two peaks at 12 and 20° corresponding to Bragg spacings of 7.4 and 4.5 Å, respectively. The last value is usually reported as the intrachain segment distance, whereas the first reflection is related to the distance between the chain segments.[12,34,42] The first peak is present in so-called mesomorphic polymeric materials, such as polysilsesquioxanes[35,42,43] or poly (diphenylsiloxane),[44,45] and its width can be related to the degree of organization of the network.[33] This peak became broader for the membranes obtained at higher temperatures (MPP4 and MPP5). Hence, the partial degradation of the organic component of these hybrid materials leads to an increase in the disorder of the network in comparison with the membranes pyrolyzed at lower temperatures. It is worth emphasizing that no sharp peaks were detectable in the XRD plots of the membranes prepared in this investigation; therefore, the partial pyrolysis did not induce the formation of crystalline phases.

SAXS

SAXS is an established technique for the morphological characterization of polymeric materials. The X-rays are scattered because of fluctuations of the electron density in the material. These fluctuations can be associated with phase separation (in copolymers[46–48]), crystallization,[49–51] the presence of particles,[31,52–58] and different crosslinking densities,[7,12] among other things.

The SAXS pattern of MPP1 was investigated in a previous publication,[31] and the curve had a peak centered at $q = 0.1$ Å^{-1}, which could be associated with a correlation distance between the clusters (nodes of the PDMS network). To investigate the morphological changes of MPP1 membranes caused by the thermal treatment, the partially pyrolyzed membranes were also characterized with SAXS. The curves are displayed in Figure 7.

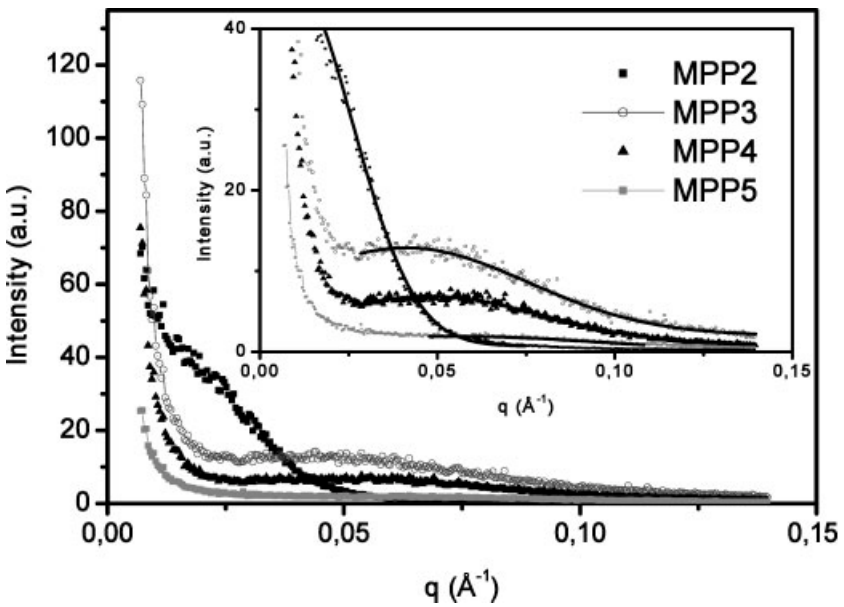

Figure 7. SAXS curves of the partially pyrolyzed membranes (the curves have been shifted vertically for the sake of clarity).

Table 3. Correlation Distance (d) and Position of the Maximum (q_{max}) of the Partially Pyrolyzed Membranes

Membrane	d (Å)	q_{max} (Å^{-1})
MPP1[31]	63	0.10
MPP2	628	0.01
MPP3	157	0.04
MPP4	126	0.05
MPP5	105	0.06

The SAXS curve of MPP2 exhibits a correlation peak, which is partially overlapped by an upturn at q values higher than 0.01 Å^{-1}. The exact position of the maximum could be determined to be 0.01 Å^{-1} by the fitting of the shoulder with a Gaussian function. As reported in previous publications, this peak can be associated with the relatively ordered array of clusters spaced by a distance d, which can be determined from the position of the maximum (q_{max}) with eq 3:

$$d = \frac{2\pi}{q_{max}} \tag{3}$$

This correlation distance is 628 Å. Therefore, the thermal treatment of MPP1 under relatively mild conditions (a purge temperature of 150 °C and an oxidation temperature of 100 °C) caused a significant change in the distance between the clusters in the PDMS network.

The membranes pyrolyzed at higher temperatures showed even more drastic morphological changes. The position of the correlation peak shifted to lower q values, and this indicated that the clusters became closer to each other for the membranes heated at higher temperatures. This fact is in line with the partial elimination of PDMS segments through thermally induced rearrangements, as discussed in the previous

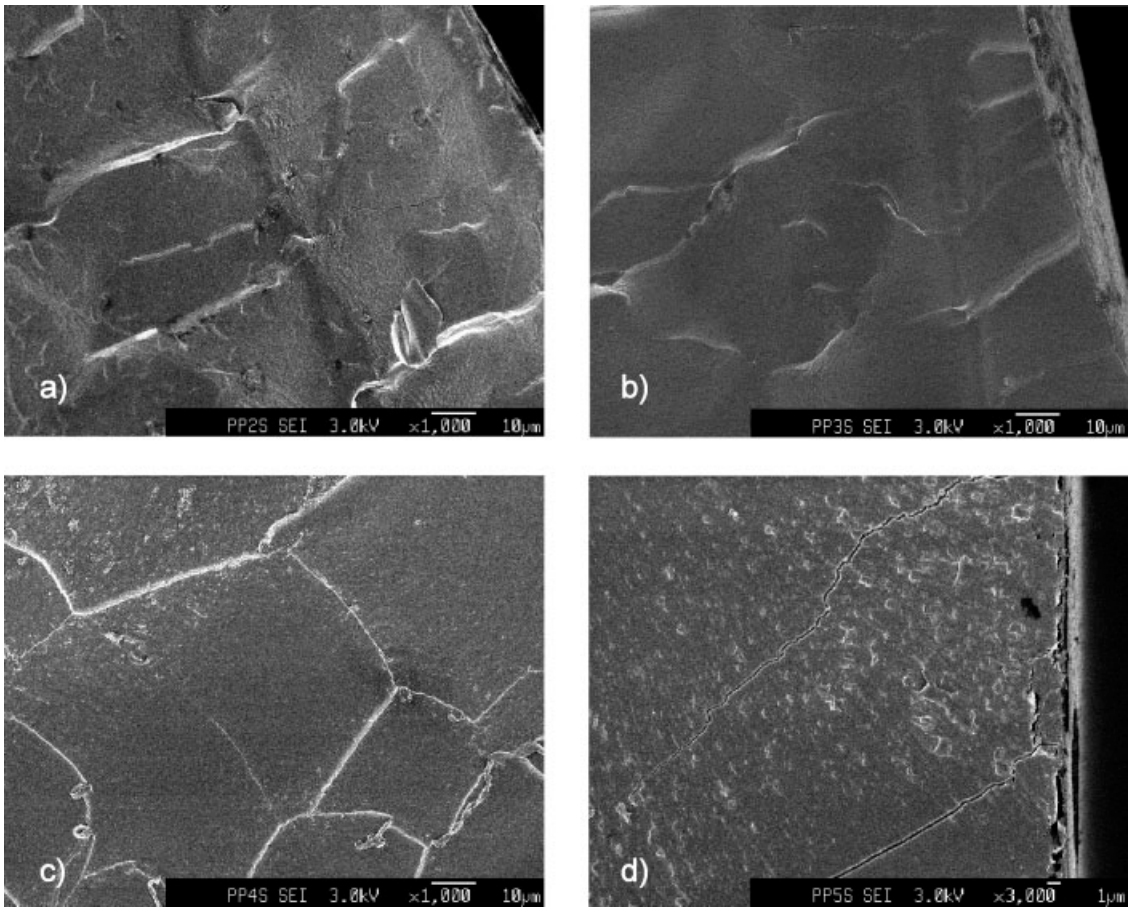

Figure 8. Surfaces of cryogenically fractured specimens: (a) MPP2, (b) MPP3, (c) MPP4, and (d) MPP5.

Table 4. Permeability Coefficients for the MPP*i* Membranes

	Permeability Coefficient (Barrer)[a]				
Membrane	N_2	H_2	O_2	CH_4	CO_2
MPP1	425 ± 7	770 ± 42	965 ± 28	1481 ± 15	2212 ± 69
MPP2	277 ± 12	532 ± 6	631 ± 25	1127 ± 18	1574 ± 23
MPP3	447 ± 2	901 ± 35	662 ± 9	1096 ± 11	3469 ± 72
MPP4	425 ± 3	455 ± 5	690 ± 9	945 ± 11	2659 ± 49
MPP5	4.6×10^4	10.0×10^4	4.1×10^4	8.1×10^4	3.6×10^4
PDMS[59]	400 ± 10	890 ± 30	800 ± 20	1200 ± 40	3800 ± 70

[a] 1 Barrer = 10^{-10} cm^3 cm/s cm^2 cmHg.

sections of this article. Furthermore, the peaks became broader and weaker for the membranes pyrolyzed at higher temperatures, and this is in line with the partial degradation of the PETA/AS organic moieties. The decrease in the intercluster distance is also supported by the increase in E' of the membranes in the viscoelastic regime. The lower the distance is between the crosslinking nodes, the higher E' is at temperatures higher than T_g. The data extracted from the SAXS analysis are reported in Table 3.

Evaluation of the Gas Permeability

Figure 8 shows micrographs of the cryogenic fracture surfaces of the membranes. In all of them, cracks were produced during the fracture. MPP1, MPP2, MPP3, and MPP4 were dense, self-supported, and crack- and defect-free films. Therefore, the permeability can be described by the classical theory developed for gas transport through dense polymeric membranes.

The permeability and selectivity coefficients of H_2, N_2, O_2, CO_2, and CH_4 of MPP1, MPP2, MPP3, MPP4, and MPP5 membranes are summarized in Tables 4 and 5, respectively. The measurements were performed with a bubble flow meter as previously described by Redondo et al.[12]

According to the data displayed in Table 4, the partially pyrolyzed membrane exhibited a behavior comparable to that of MPP1, that is, $P(CO_2) > P(CH_4) > P(O_2) > P(H_2) > P(N_2)$ (where P is the permeability coefficient), which can be understood on the basis of the predominance of linear segments of PDMS in the polymeric network.

The permeability and ideal selectivity coefficients for these membranes (including MPP1) were comparable to those reported for commercial PDMS-based membranes.[59]

CONCLUSIONS

The partial pyrolysis process revealed itself as a viable method for the preparation of crack-free, self-supported polysiloxane membranes. The Si/O ratio increased with the increase in the temperature of pyrolysis, mainly in the oxidative stage, because of the thermooxidation of organic moieties, with a consequent increase in the crosslinking density of the polymeric network. The resulting membranes clearly showed improved

Table 5. Ideal Selectivity Coefficients for the MPP*i* Membranes

	Ideal Selectivity Coefficient			
Membrane	O_2/N_2	O_2/H_2	CO_2/CH_4	CO_2/N_2
MPP1	2.3 ± 0.1	1.3 ± 0.1	1.5 ± 0.1	5.2 ± 0.3
MPP2	2.3 ± 0.1	1.2 ± 0.1	1.4 ± 0.1	5.7 ± 0.3
MPP3	1.5 ± 0.1	0.7 ± 0.1	3.2 ± 0.1	7.8 ± 0.2
MPP4	1.6 ± 0.1	1.5 ± 0.1	2.8 ± 0.1	6.3 ± 0.2
MPP5	0.9 ± 0.1	0.4 ± 0.1	0.4 ± 0.1	0.8 ± 0.1
PDMS[59]	2.0	0.9	3.2	9.5

mechanical properties and thermal stability, opening potential applicability in systems operating at relatively high temperatures. These improvements can be partially explained in terms of an increase in the crosslinking density.

The gas-transport properties and morphology of the partially pyrolyzed membranes were strongly affected by the pyrolysis conditions. No formation of crystalline phases could be observed by XRD measurements, although evidence for an increase in the disorder of the material could be obtained by both XRD and SAXS techniques. The relative amounts of clusters that stemmed from *in situ* polycondensation of PETA/AS and TEOS were lower for the membranes pyrolyzed at higher temperatures.

The Fundação de Amparo à Pesquisa do Estado de São Paulo and Coordenação de Aperfeiçoamento de Pessoal de Nível Superior are gratefully acknowledged for the financial support given to this project. The authors also thank HASYLAB and Sergio S. Funari for the SAXS measurements at Beamline A2 (project no. II-04-072).

REFERENCES AND NOTES

1. Kotliar, A. M. J Polym Sci Part D: Macromol Rev 1981, 16, 367–395.
2. Rocha, R. M.; Greil, P.; Bressiani, J. C.; Bressiani, A. H. A. Mater Sci Forum 2003, 416, 505–510.
3. Moalla, S.; Kalfat, R.; Legrand, A. P.; Zarrouk, H. J Sol-Gel Sci Technol 2003, 26, 125–129.
4. Schiavon, M. A.; Radovanovic, E.; Yoshida, I. V. P. Powder Technol 2002, 123, 232–241.
5. Wei, Q.; Pippel, E.; Woltersdorf, J.; Scheffler, M.; Greil, P. Mater Chem Phys 2002, 73, 281–289.
6. Radovanovic, E.; Gozzi, M. F.; Goncalves, M. C.; Yoshida, I. V. P. J Non-Cryst Solids 1999, 248, 37–48.
7. Pinho, R. O.; Radovanovic, E.; Torriani, I. L.; Yoshida, I. V. P. Eur Polym J 2004, 40, 615–622.
8. Xu, H. Y.; Kuo, S. W.; Huang, C. F.; Chang, F. C. J Appl Polym Sci 2004, 91, 2208–2215.
9. Erdmann, E.; Destefanis, H. A.; Abalos, R.; Frontini, P. M.; Abraham, G. A. J Appl Polym Sci 2002, 85, 1624–1633.
10. Sforca, M. L.; Yoshida, I. V. P.; Borges, C. P.; Nunes, S. P. J Appl Polym Sci 2001, 82, 178–185.
11. Osorio-Galindo, M.; Iborra-Clar, A.; Alcaina-Miranda, I.; Ribes-Greus, A. J Appl Polym Sci 2001, 81, 546–556.
12. Redondo, S. U. A.; Radovanovic, E.; Torriani, I. L.; Yoshida, I. V. P. Polymer 2001, 42, 1319–1327.
13. Chang, Y. H.; Kim, J. H.; Lee, S. B.; Rhee, H. W. J Appl Polym Sci 2000, 77, 2691–2702.
14. Lee, Y. B.; Park, H. B.; Shim, J. K.; Lee, Y. M. J Appl Polym Sci 1999, 74, 965–973.
15. Sforca, M. L.; Yoshida, I. V. P.; Borges, C. P.; Nunes, S. P. J Membr Sci 1999, 159, 197–207.
16. Dvornic, P. R.; Lenz, R. W. In High Temperature Siloxane Elastomers; Dvornic, P. R.; Lenz, R. W., Eds.; Hüthig & Wepf: Basel, Switzerland, 1990; Chapter 2.
17. Stern, S. A. J Membr Sci 1994, 94, 1–65.
18. Tang, Y.; Tsiang, R. Polymer 1999, 40, 6135–6146.
19. Brook, M. A. Silicon in Organic, Organometallic and Polymer Chemistry; Wiley: New York, 2000; Chapter 9.
20. Rajan, G. S.; Sur, G. S.; Mark, J. E.; Schaefer, D. W.; Beaucage, G. J Polym Sci Part B: Polym Phys 2003, 41, 1897–1901.
21. Soufyani, M.; Jei, T.; Bourret, D.; Sivade, A.; Larbot, A. Sep Purif Technol 2001, 25, 451–457.
22. Redondo, S. U. A.; Goncalves, M. C.; Yoshida, I. V. P. J Appl Polym Sci 2003, 89, 3739–3746.
23. Robeson, M.; Burgone, W. F.; Langsam, M.; Savoca, A. C.; Tien, C. F. Polymer 1994, 35, 4970–4978.
24. Aoki, T. Prog Polym Sci 1999, 24, 951–993.
25. Koresh, J. E.; Soffer, A. Sep Sci Technol 1987, 22, 973–982.
26. Rao, M. B.; Sircar, S. J Membr Sci 1993, 85, 253–264.
27. Saracco, G.; Verteeg, G. F.; Van Swaaij, W. P. M. J Membr Sci 1994, 95, 105–123.
28. Koresh, J. E.; Soffer, A. Sep Sci Technol 1983, 18, 723–734.
29. Stevens, N. S. M.; Rezac, M. E. Chem Eng Sci 1998, 53, 1699–1711.
30. Stevens, N. S. M.; Rezac, M. E. Polymer 1999, 40, 4289–4298.
31. José, N. M.; Prado, L. A. S. A.; Yoshida, I. V. P. J Polym Sci Part B: Polym Phys 2004, 42, 4281–4292.
32. Raman, V. J Mater Sci Lett 1993, 12, 1188–1190.
33. Zanetti, M.; Bracco, P.; Costa, L. Polym Degrad Stab 2004, 85, 657–665.
34. Werlang, M. M.; Yoshida, I. V. P.; de Araújo, M. A. J Inorg Organomet Polym 1995, 5, 75–85.
35. Prado, L. A. S. A.; Pastore, H. O.; Radovanovic, E.; Torriani, I. L..; Yoshida, I. V. P. J Polym Sci Part B: Polym Phys 2000, 38, 1580–1589.
36. Bellamy, L. J. The Infrared of Complex Molecules; Wiley: New York, 1957; Chapter 20.
37. Camino, G.; Lomakin, S. M.; Lageard, M. Polymer 2001, 42, 2011–2015.
38. Camino, G.; Lomakin, S. M.; Lazzari, M. Polymer 2001, 42, 2395–2402.
39. Schiavon, M. A.; Redondo, S. U. A.; Pina, S. R. O.; Yoshida, I. V. P. J Non-Cryst Solids 2002, 304, 92–100.
40. Ward, I. M.; Sweeney, J. An Introduction to the Mechanical Properties of Solid Polymers, 2nd ed.; Wiley: Chichester, England, 2004; Chapter 3.

41. Méle, P.; Marceau, S.; Brown, D.; de Puydt, Y.; Albérola, N. M. Polymer 2002, 43, 5577–5586.
42. Prado, L. A. S. A. Ph.D. Thesis, Universidade de Campinas, 2001.
43. Baney, R. H.; Itoh, M.; Sakakibara, A.; Suzuki, T. Chem Rev 1995, 95, 1409–1430.
44. Ganicz, T.; Stanczyk, W. A. Prog Polym Sci 2003, 28, 303–329.
45. Babchinitser, T. M.; Kazaryan, L. G.; Tartakovskaya, L. M.; Vasilenko, N. G.; Zhdanov, A. A.; Korshak, V. V. Polymer 1995, 26, 1527–1530.
46. de la Fuente, J. L.; Wilhelm, M.; Spiess, H. W.; Madruga, E. L.; Fernandez-García, M.; Cerrada, M. L. Polymer 2005, 46, 4544–4553.
47. Kwee, T.; Taylor, S. J.; Mauritz, K. A.; Storey, R. F. Polymer 2005, 46, 4480.
48. Theunissen, E.; Overbergh, N.; Reynaers, H.; Antoun, S.; Jerome, R.; Mortensen, K. Polymer 2004, 45, 1857–1865.
49. (a) Kaji, K. In Handbook of Thermoplastic Polyesters, 1st ed.; Fakirov, S., Ed.; Wiley: New York, 2002; Chapter 4, pp 227–236; (b) Matsuo, M.; Bin, Y. In Handbook of Thermoplastic Polyesters, 1st ed.; Fakirov, S., Ed.; Wiley: New York, 2002; Chapter 9, pp 227–236; (c) Denchev, Z.; Sics, I.; Nogales, A.; Esquerra, T. A. In Handbook of Thermoplastic Polyesters, 1st ed.; Fakirov, S., Ed.; Wiley: New York, 2002; Chapter 11, pp 541–543.
50. Habsuda, J.; Simon, G. P.; Cheng, Y. B.; Hewitt, D. G.; Toh, H.; Cser, F. Polymer 2002, 43, 4627–4638.
51. Habsuda, J.; Simon, G. P.; Cheng, Y. B.; Hewitt, D. G.; Toh, H. Polymer 2002, 43, 4123–4136.
52. de Almeida Prado, L. A. S.; Wittich, H.; Schulte, K.; Garamus, V. M.; Willumiet, R.; Vetter, S.; Ruffmann, B.; Nunes, S. P. J Polym Sci Part B: Polym Phys 2004, 42, 567–575.
53. de Almeida Prado, L. A. S.; Wittich, H.; Schulte, K.; Garamus, V. M.; Willumiet, R.; Ponce, M. L.; Nunes, S. P. J Polym Sci Part B: Polym Phys 2005, 43, 2981–2992.
54. Sarmento, V. H. V.; Dahmouche, K.; Santilli, C. V.; Pulcinelli, S. H.; Craievich, A. F. J Appl Crystallogr 2003, 1, 473–477.
55. Dahmouche, K.; Carlos, L. D.; Santilli, C. V.; de Zea Bermudez, V.; Craievich, A. F. J Phys Chem B 2002, 106, 4377–4382.
56. Tian, D.; Blacher, S.; Jerome, R. Polymer 1999, 40, 951–957.
57. Dahmouche, K.; Santilli, C. V.; Silva, M.; Ribeiro, C. A.; Pulcinelli, S. H.; Craievich, A. F. J Non-Cryst Solids 1999, 247, 108–113.
58. Judeinstein, P.; Titman, J.; Stamm, M.; Schmidt, H. Chem Mater 1994, 6, 127–134.
59. Merkel, T. C.; Bondar, V. I.; Nagai, K.; Freeman, B. D.; Pinau, I. J Polym Sci Part B: Polym Phys 2000, 38, 415–434.